TITLE

Recombination-independent recognition of DNA homology for meiotic silencing in *Neurospora crassa*

AUTHORS

Nicholas Rhoades[1], Germano Cecere[2], Thomas Hammond[1] and Eugene Gladyshev[3 *]

AFFILIATIONS

1. School of Biological Sciences, Illinois State University, Normal IL 61790, USA

2. Group Mechanisms of Epigenetic Inheritance, Department of Developmental and Stem Cell Biology, Institut Pasteur, Paris 75015, France

3. Group Fungal Epigenomics, Department of Mycology, Institut Pasteur, Paris 75015, France

[*] corresponding author (eugene.gladyshev@gmail.com)

ABSTRACT

Pairing of homologous chromosomes represents a key aspect of meiosis in nearly all sexually reproducing species. While meiotic pairing requires the formation of double-strand DNA breaks in some organisms, in many others it can proceed in the apparent absence of DNA breakage and recombination. The mechanistic nature of such recombination-independent pairing represents a fundamental question in molecular biology. Using “meiotic silencing by unpaired DNA” (MSUD) in the fungus *Neurospora crassa* as a model system, we demonstrate the existence of a cardinally new solution to the problem of inter-chromosomal homology recognition during meiosis. Here we take advantage of the unique ability of MSUD to efficiently detect and silence (by RNA interference) any relatively short DNA fragment lacking a homologous allelic partner. We show that MSUD does not require the function of eukaryotic RecA proteins and the type II topoisomerase-like protein Spo11. We further show that MSUD can recognize patterns of weak interspersed homology in which short units of sequence identity are arrayed with a periodicity of 11 base-pairs (bp). Taken together, these results reveal the function of a recombination-independent homology-directed process in guiding the expression of small interfering RNAs and suggest that meiotic chromosomes can be evaluated for sequence homology at base-pair resolution by a mechanism that operates on intact DNA molecules.

MAIN TEXT

Proper pairing of homologous chromosomes in meiosis is essential for ensuring fertility and preventing birth defects. While the general role of recombination during meiosis has been firmly established (1), many organisms (including the fruit fly *D. melanogaster* and the roundworm *C. elegans*) feature "non-canonical" programs in which homologous chromosomes can identify one another in the apparent absence of DNA breakage and recombination (1). Such recombination-independent pairing was previously suggested to rely on various forms of "bar-coding" by transcription, proteins, RNAs, or landmark genomic features such as centromeres and telomeres (2-6). Alternatively, there exists a possibility that recombination-independent pairing may be guided directly at the level of DNA homology (7, 8), but the experimental evidence for this type of homologous inter-chromosomal communication in meiosis remains sparse (9).

In the model fungus *Neurospora crassa*, a process known as meiotic silencing by unpaired DNA (MSUD) can identify non-homologous DNA sequences present at allelic chromosomal positions (10). Once detected, such sequences undergo transient post-transcriptional silencing by RNA interference (10). The ability of MSUD to detect non-homologous sequences as short as ~1 kbp, irrespective of nucleotide composition and transcriptional capacity, strongly suggests that a general homology search is involved (11). Furthermore, because MSUD occurs within a relatively short time interval (a few hours at the beginning of prophase I), the underlying search mechanism must be very efficient.

Previous studies have identified a substantial number of factors required for MSUD (11, 12), but they have not explored the possible connection between MSUD and meiotic recombination. The genome of *N. crassa* encodes only one RecA-like protein, MEI-3^{RAD51}, which is largely dispensable during vegetative growth but becomes essential in meiosis (13). This lethal phenotype can be fully suppressed by inactivating Spo11, a conserved type II topoisomerase-like protein that generates recombination-initiating double-strand DNA breaks (14). Thus, *N. crassa* can complete meiosis and produce viable (but frequently aneuploid) progeny in the absence of both MEI-3^{RAD51} and Spo11 (8). We took advantage of this experimental system to test if MEI-3^{RAD51} and Spo11 were required for recognition of non-homologous DNA during MSUD.

Because Spo11-deficient crosses tend to produce aberrant spores, we had to avoid using standard spore features, such as shape or color, in our analysis. Instead, we chose to assay the expression of a fluorescent fusion protein, hH1-GFP (15), directly in the meiotic cell. To create appropriate reporter strains, the *hH1-gfp* construct was integrated by homologous recombination as the replacement of the *mei-3* gene (Fig. 1A). When the construct is provided by the female parent, many additional nuclei in the fruiting body are expected to express hH1-GFP. Alternatively, when the construct is provided by the male parent, hH1-GFP expression should be restricted to the generative lineage comprising premeiotic, meiotic and postmeiotic

nuclei. To preclude the *hH1-gfp* construct from being inactivated in premeiotic nuclei by repeat-induced point mutation (RIP), crosses were performed in appropriate RIP-deficient genetic backgrounds (16, 17).

We first analyzed a cross in which meiotic recombination and MSUD remained functional, while only one copy of *mei-3::hH1-gfp* was present in the diploid nucleus (Fig. 1B and 1C: *mei-3+/Δ, spo11+/+*). As expected, no meiotic expression of hH1-GFP was observed. This result was obtained regardless of whether the reporter construct was provided by the female or the male parent. The expression of hH1-GFP in this heterozygous condition could be readily restored by the partial attenuation of MSUD (Fig. 1C: *mei-3+/Δ, spo11+/Δ, sad-2+/Δ*). This suppression effect was achieved by using a dominant deletion allele of *sad-2* (11). Taken together, these results indicate that the *mei-3::hH1-gfp* reporter provides a reliable readout of MSUD activity.

We next asked if *mei-3::hH1-gfp*, when present in only one copy, was detected by MSUD in the complete absence of MEI-3^{RAD51} and Spo11. Here we analyzed a *spo11Δ/Δ* cross in which the reporter construct was matched against a standard *mei-3Δ* deletion allele produced by the Neurospora Genome Project (18). We found that the *mei-3::hH1-gfp* allele was fully silenced in this situation (Fig. 1C: *mei-3Δ/Δ, spo11Δ/Δ*, "unpaired" *hH1-gfp*). The expression of hH1-GFP was restored when two identical *mei-3::hH1-gfp* alleles were provided (Fig. 1C: *mei-3Δ/Δ, spo11Δ/Δ*, "paired" *hH1-gfp*). Taken together, these results demonstrate that MSUD remains functional in the absence of MEI-3^{RAD51} and Spo11.

While Spo11 is required for normal levels of meiotic pairing in *N. crassa* (19), residual Spo11-independent recombination has also been reported (20). To investigate if such non-canonical recombination could have occurred in our *spo11Δ/Δ* crosses, we examined the level of linkage between two widely-separated genetic markers, *mat a* and *csr-1Δ*, on Chromosome I (Fig. 1D). Notably, this interval includes the *his-3* locus, which was previously shown to exhibit substantial levels of Spo11-independent recombination in crosses between certain *Neurospora* strains (19, 20). We used the *csr-1Δ* marker for the following reasons: (i) only loss-of-function *csr-1* alleles can confer resistance to cyclosporin A, (ii) this resistance is recessive, and (iii) *csr-1+* remains stable during the sexual phase (17). Thus, following a *csr-1+/Δ* cross, partial diploids with two different Chromosomes I (produced by nondisjunction in meiosis I and corresponding to the genotype *csr-1+/Δ*) can be avoided by germinating spores on cyclosporin-containing medium. Through this approach, we selectively isolated *csr-1Δ* progeny and performed additional genotyping at the *mat* locus with a PCR-based assay, which was specifically designed to detect a potential mixture of *mat A* and *mat a* DNA (Methods).

We started by examining a *mei-3Δ/Δ, spo11Δ/Δ* cross that had already been assayed for MSUD (Fig. 1D; Supplementary Table 2: cross "X5"). Analysis of 513 *csr-1Δ* progeny of this cross failed to identify a single instance of the recombinant genotype *mat A, csr-1Δ* (Fig. 1D). As a control, we also examined the degree of linkage between *mat a* and *csr-1Δ* in a *mei-3+/Δ, spo11+/Δ* cross, in which meiotic recombination was at least partially active (Fig. 1D, Supplementary Table 2: cross "X9"). A substantial proportion of recombinant progeny was recovered (26%, Fig. 1D: *mei-3+/Δ, spo11+/Δ*), demonstrating that our assay was sensitive enough to detect recombination even in this sub-optimal situation (*i.e.*, when both MEI-3^{RAD51} and Spo11 were expressed from single "unpaired" *mei-3+* and *spo11+* alleles, respectively). These results provided additional evidence that MSUD remains functional in the absence of recombination.

In metazoans, a phenomenon known as "meiotic silencing of unsynapsed chromatin" (MSUC) occurs in concert with the trimethylation of histone H3 lysine-9 (H3K9me3) over long unpaired chromosomal regions (21). Thus, it was important to investigate if H3K9me3 was required for MSUD. In *N. crassa,* H3K9me3 is mediated by a SUV39 lysine methyltransferase DIM-5 (22). While *Neurospora dim-5Δ* strains are largely infertile as females, this defect can be suppressed by the deletion of SET-7, a lysine methyltransferase that mediates trimethylation of histone H3 lysine-27 (H3K27me3) in the context of facultative heterochromatin (23, 24). To simultaneously test the roles of both H3K9me3 and H3K27me3, we assayed silencing of the *mei-3::hH1-gfp* reporter in a *dim-5Δ/Δ, set-7Δ/Δ* cross. We found that, when *mei-3::hH1-gfp* was matched against *mei-3+*, the expression of hH1-GFP in the meiotic nucleus was completely silenced (Supplementary Fig. 1), suggesting that MSUD is not impeded by the concomitant absence of DIM-5 and SET-7. These results demonstrate that, unlike MSUC in metazoans, MSUD does not require the formation of H3K9me3.

The ability of MSUD to function normally in the absence of MEI-3^{RAD51} and Spo11 was surprising. Yet, it is not the first discovery of a general recombination-independent homology-recognition process in *N. crassa*. For example, RIP (introduced above) is activated in the haploid nuclei that divide by mitosis several times in preparation for karyogamy and meiosis (16). The most remarkable feature of RIP is its ability to detect gene-sized DNA repeats largely irrespective of their type (*e.g.*, transposable element, intergenic DNA, or protein-coding gene), origin, transcriptional capacity, or positions in the genome (16). Our previous work has shown that RIP senses repeats by a mechanism that does not require MEI-3^{RAD51} and Spo11 (8). We also found that RIP can detect instances of weak but periodic homology, in which homologous segments of 3 bp or longer are interspersed with a periodicity of 11 or 12 bp (8). These prior results suggested that RIP recognizes homology directly between intact DNA molecules, by matching them as arrays of interspersed base-pair triplets (8). Given that MSUD also involves a recombination-independent mechanism, we next asked if this mechanism is capable of sampling interspersed homology.

We started by developing a robust experimental system to dissect the ability of MSUD to recognize weak interspersed homology. We refer to a pattern of interspersed homology as "weak" if it corresponds to an overall sequence identity of 50% or less. We chose to use a *Roundspore* (*Rsp*)-based assay as a genetic reporter of MSUD (11). In this assay, a promoter-less 1370-bp fragment of the *Rsp* gene, placed at an ectopic position and lacking an allelic copy, triggers MSUD-mediated silencing of the endogenous *Rsp+* alleles (Fig. 2A,B). As a result, the spore shape is altered from spindle-like to round (11). This change can be quantified by estimating the fraction of spindle-shaped spores in a relatively large sample of randomly discharged products (Methods). Using the 1370-bp *Rsp* fragment as a reference sequence (herein referred to as "Ref"), we designed a series of 1370-bp synthetic sequences, each with a different pattern of interspersed homology with respect to Ref. Analyzed patterns had an overall format of **X**H-**Y**N, where **X**-bp units of homology were separated by **Y**-bp units of non-homology (8). All tested patterns are provided in Fig. 2C. Each test sequence was inserted together with a Hygromycin B-resistance marker near *his-3* (Fig. 2A).

We started by analyzing a set of crosses in which each Ref/Test pair was surrounded by perfect homology (Fig. 2D: left panel). In this situation, even the case of *zero* homology corresponded to ~74% of spindle-shaped spores, suggesting that MSUD often failed to detect the absence of homology. This result contrasts with the case of physically deleted DNA analyzed in the same experiment (Fig. 2D: left panel, "Del"). The basis for this disparity remains unclear, but it may involve the formation of qualitatively different chromatin structures depending on whether the participating sequences could form a co-linear pair. Nevertheless, these results provided a hint that weak interspersed homology (including patterns *4H-7N* and *3H-8N_4*, corresponding to the overall identity of 36.4% and 27.3%, respectively) could be efficiently recognized by MSUD.

We next sought to enhance the sensitivity of our assay. We reasoned that creating a region of non-homology (or random homology) next to the assayed region would improve the ability of MSUD to discriminate between Ref and Test sequences. To this end, the HygR region in the Ref construct was replaced with an unrelated fragment of *E. coli* genomic DNA of the same length (termed "*E. coli* spacer DNA" or Ecs). Indeed, in this new system, the fraction of spindle-shaped spores corresponding to *zero* homology decreased to 37% (Fig. 2D: central panel). Overall, the results of these experiments support several conclusions. First, interspersed homologies with a periodicity of 11 bp and an overall sequence identity as low as 36.4% (*i.e.*, pattern *4H-7N*) are recognized by MSUD as fully homologous (these effects could also be confirmed in the intact asci, Supplementary Fig. 2). Second, not every interspersed homology can be recognized in principle (*i.e.*, pattern *2H-1N*, 66.7% sequence identity), demonstrating that the overall amount of homology is less important than its arrangement. Third, a triplet of base-pairs constitutes the minimally effective recognition unit. Fourth, not all identical patterns of interspersed homology are recognized with the same efficiency

(*i.e.*, patterns *3H-8N* vs. *3H-8N_4*). Fifth, increasing the periodicity of interspersed homology beyond 22 bp interferes with its recognition by MSUD (i.e., patterns *11H-11N* vs. *11H-22N*).

As a control, we also examined the ability of our Test sequences to silence the endogenous *Rsp+* alleles in crosses lacking the Ref construct (Fig. 2D: right panel). We found that only the Test sequence with perfect homology to *Rsp+* (*i.e.*, the Ref sequence itself) was able to trigger MSUD when matched against a deletion (*i.e.*, wildtype DNA), indicating that all other Test sequences are insufficient for *Rsp* silencing.

Having discovered the ability of MSUD to recognize weak interspersed homology, we next sought to extend this observation at the molecular level by analyzing the expression of MSUD-associated small interfering RNAs (masiRNAs), which are produced during meiosis from regions of allelic non-homology (25, 26). To this end, we used the above reporter system containing the Ecs/HygR region as an instance of permanent non-homology (Fig. 3A). We first analyzed a cross in which the Ref/Test regions comprised the case of *zero* homology (Fig. 3B: cross "P1 x P2"). Importantly, while the Ref region corresponded to an endogenous sequence (the *Rsp* gene), the sequence in the Test region ("*zero*") was produced by a random-number generator. Still, potent expression of masiRNAs was observed for all analyzed regions (Fig. 3B: cross "P1 × P2"; HygR-specific masiRNAs were excluded from analysis because HygR was also present at unrelated genomic positions in these crosses, Supplementary Table 1 and 2). These results suggest that the expression of masiRNAs can be used as a powerful reporter of DNA homology recognition during meiosis in *N. crassa*. We next examined two instances of interspersed homology: *7H-4N* and *4H-7N* (Fig. 3B: crosses "P1 × P3" and "P1 × P4", respectively). Strikingly, the expression of masiRNAs from the Ref/Test region was essentially abolished in both cases, except for a relatively small amount of masiRNAs immediately adjacent to Ecs/HygR in the case of *4H-7N*.

We performed two additional experiments to further explore the idea that the expression of masiRNAs in our experimental system is guided by homology recognition. Our results (above) showed that the *4H-7N* region did not induce MSUD when matched against the Ref region. In principle, the absence of masiRNAs in this situation could be attributed to unanticipated features associated with the design of this synthetic sequence. To test if the *4H-7N* sequence can support the expression of masiRNAs in principle, we crossed the same *4H-7N*-carrying strain with a mating partner in which the Ref sequence was replaced with the *zero* sequence (Fig. 3B: cross "P5 × P4"). The *4H-7N* and *zero* sequences were independently designed using Ref as a template, and as a result, they have an overall identity of 19.7% and comprise an instance of nearly random homology. As such, they were expected to trigger MSUD. This prediction was confirmed by the detection of masiRNAs corresponding to both sequences (Fig. 3B: cross "P5 × P4").

Finally, to confirm that the *zero* sequence is not a substrate for a small-RNA-generating process unrelated to MSUD, we examined a cross in which two identical *zero* sequences were present at allelic positions (Fig. 3B: cross "P5 x P2"). This cross involved the same two *zero*-carrying strains as above. As expected, very few masiRNAs were produced from the matching *zero* regions. Taken together, these results show that a recombination-independent homology-directed process can guide the expression of small interfering RNAs.

The availability of many masiRNAs corresponding to the Ecs region (4,818 aligned reads, obtained by the five independent experiments in Fig. 3B) prompted us to analyze their basic properties in more detail. The Ecs region was particularly interesting because it was taken from a bacterial genome and, therefore, could only support the production of "primary" masiRNAs (as opposed to those originating from degradation of cleaved mRNAs). Consistent with previous reports (25, 26), the number of masiRNAs expressed in the sense orientation was roughly equal to the number of masiRNAs expressed in the antisense orientation (2,576 and 2,242 reads, respectively; also plotted in Supplementary Fig. 3A). The size distribution of these masiRNAs also agreed with the previously reported values, with a characteristically skewed peak around 24-25 nt (Supplementary Fig. 3B: right panel). This distribution closely approximates the one for "genome-wide" small RNAs (24,364,806 aligned reads in total, Supplementary Fig. 3B: left panel). The apparent similarity between the Esc-derived and the genome-wide pools of small RNAs was further extended to the 5' uridine bias, which could be observed across the entire size range (Supplementary Fig. 3C).

In summary, our results reveal the existence of a cardinally new meiotic process by which sequence identity can be evaluated between chromosomes at a base-pair resolution. This process is general with respect to its capacity to detect DNA homology *per se*, does not require the function of RecA proteins or Spo11, and can efficiently detect the presence of relatively low levels of interspersed homology. The mechanistic nature of how DNA homology is sensed in this situation remains an open question. In principle, recognition may occur directly between intact DNA double helices (8, 27). In one such model (Fig. 3C), non-homologous ("unpaired") DNA can be defined by the lack of proper pairing in the context of the transiently paired chromosomal segments. This process would likely require a coordinated action of many additional factors, including Topoisomerase II (27).

Direct dsDNA-dsDNA pairing is likely impeded by strong pre-existing interactions between DNA and other factors (i.e., histones). Yet this apparent obstacle is not insurmountable. For example, a substantial fraction of histones can be removed by proteolysis in response to DNA damage, presumably to facilitate DNA repair by homologous recombination (28). Interestingly, significant proteasome-mediated protein turnover takes place on meiotic chromosomes, where it has been implicated as a necessary step in homologous pairing and recombination (29, 30).

The apparent similarity between MSUD and RIP with respect to the underlying mechanism of homology recognition is intriguing. While RIP occurs in premeiotic haploid nuclei over the course of several days and features an exhaustive genome-wide homology search, MSUD needs to operate on replicated homologous chromosomes within a narrow time interval at the beginning of the first meiotic prophase. Yet MSUD and RIP apparently rely on the same recombination-independent approach to cross-matching DNA sequences, suggesting that the same approach may be involved in a wider range of homology-directed phenomena.

METHODS

Designing reporter DNA sequences

Synthetic DNA sequences were engineered exactly as previously described (8). The *E. coli* spacer (Ecs) corresponds to the positions 1637342-1638753 of the *E. coli* genome (strain DH10B, accession CP000948). The sequence of *hH1-gfp* (including the *ccg-1* promoter) was taken from pMF280 (31).

Manipulation of *Neurospora* strains

Neurospora strains used in this study are listed in Supplementary Table 1. Vogel's Minimal medium with 1.5% sucrose was used for vegetative growth. Transformations were performed by electroporating linear plasmid DNA into macroconidia as previously described (8). Annotated sequences of all plasmids created in this study are provided in Supplementary Data File 1. Crosses were performed on Synthetic Crossing (SC) medium with 1.5% sucrose, as previously described (8). All crosses analyzed in this study are listed in Supplementary Table 2.

Assaying hH1-GFP expression

The 6-day-old perithecia were fixed in a solution of 100 mM PIPES (pH 6.9), 10 mM EGTA, 5 mM $MgSO_4$ and 4% paraformaldehyde for 20 minutes at room temperature as previously described (32). Perithecia were subsequently washed and stored in sodium phosphate buffer (80 mM Na_2HPO_4 + 20 mM NaH_2PO_4). Asci were dissected in 25% glycerol (on a microscope slide) and transferred into a drop of mounting medium containing 25% glycerol, 10 mg/mL DABCO, 5 µg/mL Hoechst 33342, and 100 mM potassium phosphate buffer at pH 8.7. Cover slips were placed over samples and sealed with a thin layer of nail polish. Slides were stored at -20ºC, if nessesary. A Leica DMBRE compound microscope with a 40x objective and the DFC300 FX camera was used for imaging. Raw images are provided in Supplementary Data File 2.

Assaying recombination

The reporter strain C194.3 (used as female) was crossed with either C50.3 or RNR136.9 (Supplementary Table 1). Spores were collected from 4-week-old crosses and plated directly on sorbose agar containing cyclosporin A. Genomic DNA was extracted from each spore clone as described previously (8). The *mat* genotype was determined by multiplex PCR with a combination of two primer pairs: one pair for *mat A* (5'-AAGTATCGCCAAAGCTGGTTC-3' and 5'-TCATGGCAAAGTCCAACTTCC-3'), and the other pair for *mat a* (5'-TCCCGGACTTCACAATAACGA-3' and 5'-GCGCGAAGTTTTCTAGATCCT-3'). One negative control ("no DNA") and two positive controls (genomic DNA of both parental strains) were included in each set of reactions prepared from a common master mix. PCR products were resolved on 1% agarose gels containing ethidium bromide. Gels were scanned using Gel Doc EZ System (Bio-Rad). All raw gel scans are provided in Supplementary Data File 3.

Assaying *Roundspore* phenotype

The *Roundspore* phenotype was quantified as described previously (33). Reporter strains (RAB10.47, RNR95.10.3, or RTH1005.2; Supplementary Table 1) were pre-grown on SC media in 60-mm culture plates for 6 days. Macroconidia of each test strain were suspended in sterile water, spore counts were performed with a hemocytometer, and concentrations were adjusted to 1000 conidia/µL. Ascospores were collected from the lids of the crossing plates 21 days after fertilization and phenotyped on a hemocytometer. For each cross, at least 1000 ascospores were analyzed. All experiments were performed and quantified in triplicate.

Preparing and sequencing small RNA libraries

Total RNA was extracted from 6-day-old perithecia with TRI Reagent (Sigma-Aldrich, T9424) and additionally purified with the Plant/Fungi Total RNA Purification Kit (Norgen Biotek, E4913). RNA was determined to have a RIN value of at least 8.0 with a TapeStation 2200 (Agilent Genomics). Total RNA was fractionated on a 15% TBE-Urea gel (ThermoFisher, EC6885BOX) to isolate RNA molecules in the 17-26 nt range. Excised small RNA-containing gel slices were incubated overnight in 0.3 M NaCl at 25°C while shaking at 650 rpm. Gel fragments were separated from the RNA-containing solution with a 0.22 µm Corning spin column (Sigma-Aldrich, CLS8161). Small RNAs were then precipitated with four volumes of 100% ethanol and isolated by centrifugation at 13000 ×g for 45 minutes at 4°C. RNA pellets were washed in 80% ethanol before resuspension in nuclease-free water. Purified small RNAs were treated with RNA 5'-polyphosphatase (Lucigen, RP8092H) to remove 5' phosphates. Resultant small RNAs were purified using 1.8 volumes of Agencourt RNAClean XP Beads (Beckman Coulter, NC0068576) and three volumes of isopropanol. The libraries were constructed as previously described (34), except that purification was performed with Agencourt RNAClean XP Beads. Libraries were quantified using a Qubit Fluorometer High

Sensitivity dsDNA assay kit (ThermoFisher, Q32851) and sequenced on an Illumina MiniSeq platform at the 76-nt read length.

Small RNA sequence analysis

Illumina reads in FASTQ format were pre-processed using the FASTX-Toolkit. Retained reads were mapped to the *N. crassa* genome assembly (accession AABX03000000.3) using Bowtie 2 version 2.3 (without allowing any mismatches in the seed alignment). A custom genome assembly containing a specific combination of the assayed sequences was created for each analyzed condition using Artemis version 16. All custom assemblies are provided in FASTA format in Supplementary Data File 4. SAM and BAM files were manipulated with SAMtools version 1.7. Aligned reads in BAM format are provided in Supplementary Data File 5. The identification of reads aligning uniquely to the assayed sequences was performed using SAMtools. Figures displaying the distribution of aligned masiRNAs, their size, 5' bias, and strand specificity were made in R version 3.4 and post-processed in GIMP.

ACKNOWLEDGMENTS

We thank Sarah Bellout, Amy Boyd, Tyler Malone, Pennapa Manitchotpisit, Turner Reid, Pegan Sauls, and Aykhan Yusifov for technical assistance during early stages of this project. The work was supported by grants from the Agence Nationale de la Recherche (10-LABX-0062) and the National Institutes of Health (1R15HD076309-01).

SUPPLEMENTARY DATA

Supplementary Data File 1. Plasmids used in this study. Annotated sequences are provided in GenBank format.

Supplementary Data File 2. Analysis of hH1-GFP expression. Raw images of dissected asci are provided in TIFF format.

Supplementary Data File 3. Analysis of recombination using PCR. Raw images of agarose gels are provided in TIFF format.

Supplementary Data File 4. Custom genome assemblies. Sequences are provided in FASTA format. Each file contains a single metacontig that corresponds to a cross analyzed in Fig. 3B.

Supplementary Data File 5. Aligned small RNA reads. Alignments are provided in BAM format. Each alignment corresponds to a cross analyzed in Fig. 3B.

DATA AVAILABILITY

Prior to peer-reviewed publication of this manuscript, all Supplementary Data Files are available from the authors upon request.

FIGURE LEGENDS

Figure 1. MSUD functions in the absence of meiotic recombination

(A) Fluorescent reporter construct contains the following parts: (i) coding sequence for the hH1-GFP fusion protein and the *ccg-1* promoter (green), (ii) Hygromycin B-resistance marker (pink), and (iii) spacer DNA corresponding to the *Rsp+* fragment analyzed in Fig. 2 (blue). The construct was designed to replace *mei-3* by homologous recombination.

(B) Over-expressed hH1-GFP accumulates in the meiotic nucleus, with higher concentrations found in the nucleolus. Expression of hH1-GFP can be silenced by MSUD if the reporter construct lacks a homologous allelic partner during meiosis.

(C) Silencing of the reporter construct was assayed in several conditions, as indicated. For each condition, the left and right panels show fluorescence signal corresponding to GFP and Hoechst 33342, respectively. Each condition represents a different cross (see Supplementary Table 2 for details). Cross identifiers are as follows, from left to right: (top) X1, X3, X5, and X7; (bottom) X2, X4, X6, and X8.

(D) Recombination between *mat a* and *csr-1Δ* was examined in two genetic conditions, as indicated. Cross identifiers are X9 (*mei-3+/Δ, spo11+/Δ*) and X5 (*mei-3Δ/Δ, spo11Δ/Δ*).

Figure 2. MSUD recognizes triplet-containing interspersed homologies

(A) Genetic reporter system is used to evaluate the ability of MSUD to recognize homology in the Ref/Test region, as indicated.

(B) If a particular Ref/Test combination is perceived as homologous, no MSUD is induced, *Rsp+/+* alleles are expressed normally, and spindle-shaped spores are produced. Alternatively, if a Ref/Test combination is perceived as non-homologous, *Rsp+/+* expression is silenced by MSUD, and round spores are produced.

(C) Analyzed patterns homology. Each pattern is formed by a particular combination of the invariable Ref region (corresponding to a promoter-less segment of *Rsp+*) and a Test region (the sequence of which can be varied as desired).

(D) The fraction of spindle-shaped spores (reflecting the situation of successfully detected homology) was determined in the three separate sets of crosses. Each cross was analyzed in triplicate. The ranges of cross identifiers are as follows (from left to right): X11 - X22 (left panel), X23 - X34 (central panel), and X35 - X46 (right panel).

Figure 3. Expression of MSUD-associated small interfering RNAs is entirely homology-directed

(A) Expression of masiRNAs is assayed in a system described in Fig. 2. The homology state of the Ref/Test region can be manipulated by changing either Ref or Test.

(B) The five related conditions are examined. Each condition corresponds to a particular cross. The range of cross identifiers (from top to bottom) is X47 - X51 (Supplementary Table 2).

(C) Non-homologous DNA is identified in the context of homologous chromosomal segments engaged in transient recombination-independent pairing interactions.

Supplementary Figure 1. MSUD does not require the formation of H3K9me3 and H3K27me3.

The roles of H3K9me3 and H3K27me3 in MSUD are examined using the same approach as in Fig. 1. The reporter construct is provided by the female parent. Three representative views are shown. The genotype of the cross is indicated on the top and corresponds to the identifier X10 (Supplementary Table 2).

Supplementary Figure 2. *Rsp* phenotype is observed in populations of random spores or intact asci

(A) Dissected asci corresponding to the four critical cases of homology examined in Fig. 2D (central panel). Cross identifiers are as follows: X24 (*perfect* homology), X25 (*7H-4N* homology), X28 (*4H-7N* homology), and X34 (*zero* homology). Three representative views are provided for each cross.

(B) Random spores for the same four crosses (above). Two representative views are provided.

Supplementary Figure 3. Basic properties of masiRNAs expressed from an exogenous DNA region

(A) Ecs-derived masiRNAs do not show any oblivious strand preference.

(B) The size distribution of Ecs-derived masiRNAs (4,818 aligned reads) approximates the size distribution of all small RNAs (24,364,806 aligned reads) obtained for the five examined conditions (Fig. 3B)

(C) The 5' uridine bias is observed in both the Esc-derived and the genome-wide pools of small RNAs across the entire size range (18-26 nt).

Supplementary Table 1. Neurospora strains used in this study.

Supplementary Table 2. Crosses analyzed in this study.

REFERENCES

1. Zickler, D. & Kleckner, N. A few of our favorite things: Pairing, the bouquet, crossover interference and evolution of meiosis. *Semin. Cell Dev. Biol.* **54**, 135–148 (2016).
2. Ding, D.-Q. *et al.* Meiosis-specific noncoding RNA mediates robust pairing of homologous chromosomes in meiosis. *Science* **336**, 732–736 (2012).

3. Ishiguro, K.-I. *et al.* Meiosis-specific cohesin mediates homolog recognition in mouse spermatocytes. *Genes Dev.* **28**, 594–607 (2014).
4. Cook, P. R. The transcriptional basis of chromosome pairing. *J. Cell. Sci.* **110**, 1033–1040 (1997).
5. Stewart, M. N. & Dawson, D. S. Changing partners: moving from non-homologous to homologous centromere pairing in meiosis. *Trends Genet.* **24**, 564–573 (2008).
6. Klutstein, M. & Cooper, J. P. The Chromosomal Courtship Dance-homolog pairing in early meiosis. *Curr. Opin. Cell Biol.* **26**, 123–131 (2014).
7. McGavin, S. A model for the specific pairing of homologous double-stranded nucleic acid molecules during genetic recombination. *Heredity (Edinb)* **39**, 15–25 (1977).
8. Gladyshev, E. & Kleckner, N. Direct recognition of homology between double helices of DNA in *Neurospora crassa*. *Nat Commun* **5**, 3509 (2014).
9. Barzel, A. & Kupiec, M. Finding a match: how do homologous sequences get together for recombination? *Nat. Rev. Genet.* **9**, 27–37 (2008).
10. Shiu, P. K., Raju, N. B., Zickler, D. & Metzenberg, R. L. Meiotic silencing by unpaired DNA. *Cell* **107**, 905–916 (2001).
11. Hammond, T. M. Sixteen Years of Meiotic Silencing by Unpaired DNA. *Adv. Genet.* **97**, 1–42 (2017).
12. Xiao, H., Hammond, T. M. & Shiu, P. K. T. Suppressors of Meiotic Silencing by Unpaired DNA. *Noncoding RNA* **5**, (2019).
13. Cheng, R., Baker, T. I., Cords, C. E. & Radloff, R. J. mei-3, a recombination and repair gene of *Neurospora crassa*, encodes a RecA-like protein. *Mutat. Res.* **294**, 223–234 (1993).
14. Lam, I. & Keeney, S. Mechanism and regulation of meiotic recombination initiation. *Cold Spring Harb Perspect Biol* **7**, a016634 (2014).
15. Alexander, W. G. *et al.* DCL-1 colocalizes with other components of the MSUD machinery and is required for silencing. *Fungal Genet. Biol.* **45**, 719–727 (2008).
16. Selker, E. U. Premeiotic instability of repeated sequences in *Neurospora crassa*. *Annu. Rev. Genet.* **24**, 579–613 (1990).
17. Gladyshev, E. & Kleckner, N. DNA sequence homology induces cytosine-to-thymine mutation by a heterochromatin-related pathway in *Neurospora*. *Nat. Genet.* **49**, 887–894 (2017).
18. Colot, H. V. *et al.* A high-throughput gene knockout procedure for *Neurospora* reveals functions for multiple transcription factors. *Proc. Natl. Acad. Sci. U.S.A.* **103**, 10352–10357 (2006).
19. Bowring, F. J., Yeadon, P. J., Stainer, R. G. & Catcheside, D. E. A. Chromosome pairing and meiotic recombination in *Neurospora crassa* spo11 mutants. *Curr. Genet.* **50**, 115–123 (2006).
20. Bowring, F. J., Yeadon, P. J. & Catcheside, D. E. A. Residual recombination in Neurospora crassa spo11 deletion homozygotes occurs during meiosis. *Mol. Genet. Genomics* **288**, 437–444 (2013).
21. Turner, J. M. A. Meiotic Silencing in Mammals. *Annu. Rev. Genet.* **49**, 395–412 (2015).

22. Rountree, M. R. & Selker, E. U. DNA methylation and the formation of heterochromatin in *Neurospora crassa*. *Heredity (Edinb)* **105**, 38–44 (2010).
23. Jamieson, K., Rountree, M. R., Lewis, Z. A., Stajich, J. E. & Selker, E. U. Regional control of histone H3 lysine 27 methylation in *Neurospora*. *Proc. Natl. Acad. Sci. U.S.A.* **110**, 6027–6032 (2013).
24. Basenko, E. Y. *et al.* Genome-wide redistribution of H3K27me3 is linked to genotoxic stress and defective growth. *Proc. Natl. Acad. Sci. U.S.A.* **112**, E6339-6348 (2015).
25. Hammond, T. M. *et al.* Identification of Small RNAs Associated with Meiotic Silencing by Unpaired DNA. *Genetics* **194**, 279–284 (2013).
26. Wang, Y., Smith, K. M., Taylor, J. W., Freitag, M. & Stajich, J. E. Endogenous Small RNA Mediates Meiotic Silencing of a Novel DNA Transposon. *G3 (Bethesda)* **5**, 1949–1960 (2015).
27. Mazur, A. K. Homologous Pairing between Long DNA Double Helices. *Phys. Rev. Lett.* **116**, 158101 (2016).
28. Hauer, M. H. *et al.* Histone degradation in response to DNA damage enhances chromatin dynamics and recombination rates. *Nat. Struct. Mol. Biol.* **24**, 99–107 (2017).
29. Ahuja, J. S. *et al.* Control of meiotic pairing and recombination by chromosomally tethered 26S proteasome. *Science* **355**, 408–411 (2017).
30. Rao, H. B. *et al.* A SUMO-ubiquitin relay recruits proteasomes to chromosome axes to regulate meiotic recombination. *Science* **355**, 403–407 (2017).
31. Freitag, M., Hickey, P. C., Raju, N. B., Selker, E. U. & Read, N. D. GFP as a tool to analyze the organization, dynamics and function of nuclei and microtubules in *Neurospora crassa*. *Fungal Genet. Biol.* **41**, 897–910 (2004).
32. Samarajeewa, D. A. *et al.* An RNA Recognition Motif-Containing Protein Functions in Meiotic Silencing by Unpaired DNA. *G3 (Bethesda)* **7**, 2871–2882 (2017).
33. Samarajeewa, D. A. *et al.* Efficient detection of unpaired DNA requires a member of the rad54-like family of homologous recombination proteins. *Genetics* **198**, 895–904 (2014).
34. Jayaprakash, A. D., Jabado, O., Brown, B. D. & Sachidanandam, R. Identification and remediation of biases in the activity of RNA ligases in small-RNA deep sequencing. *Nucleic Acids Res.* **39**, e141 (2011).
35. Hammond, T. M. *et al.* Fluorescent and bimolecular-fluorescent protein tagging of genes at their native loci in *Neurospora crassa* using specialized double-joint PCR plasmids. *Fungal Genet. Biol.* **48**, 866–873 (2011).

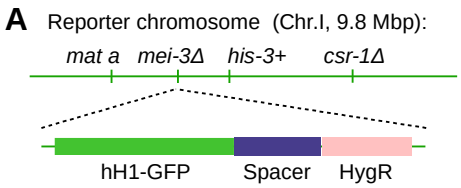

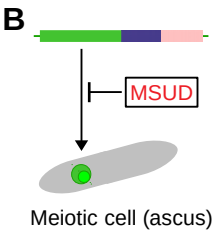

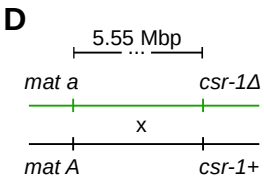

Parental (cross) genotypes	csr-1Δ progeny mat A	csr-1Δ progeny mat a
mei-3+/Δ, spo11+/Δ	26	74
mei-3Δ/Δ, spo11Δ/Δ	0	513

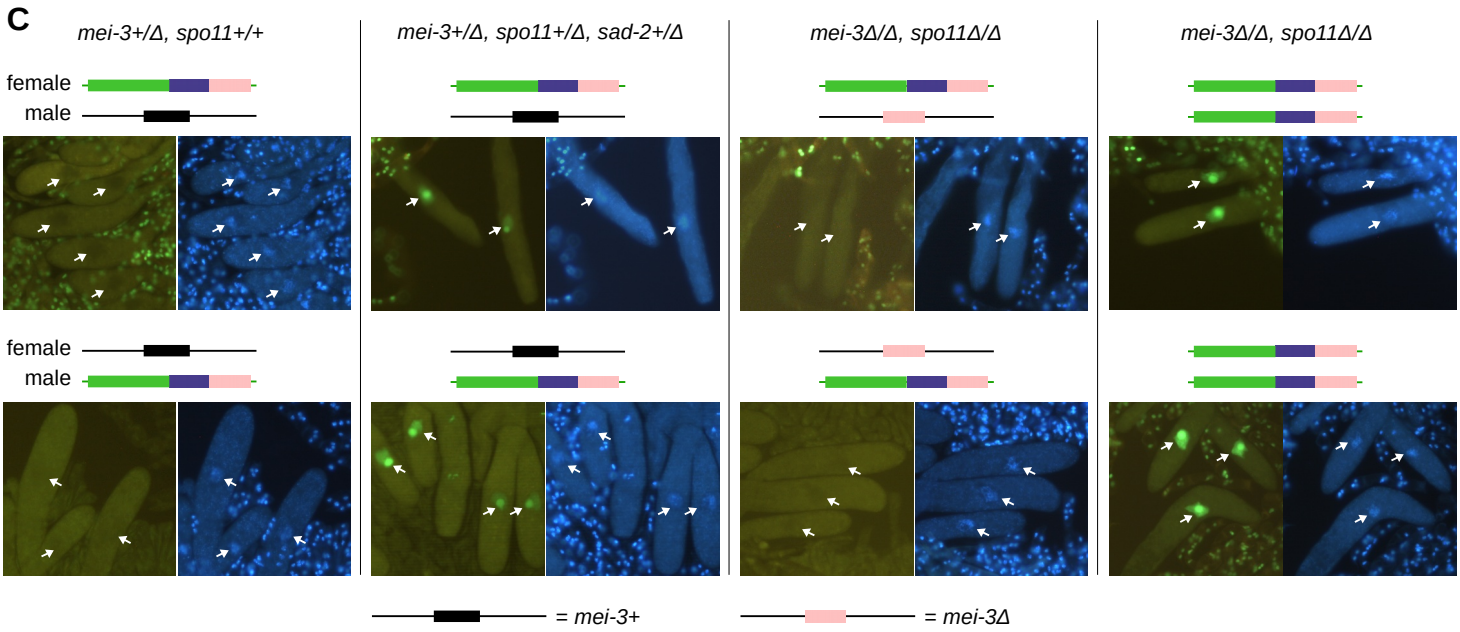

Figure 1

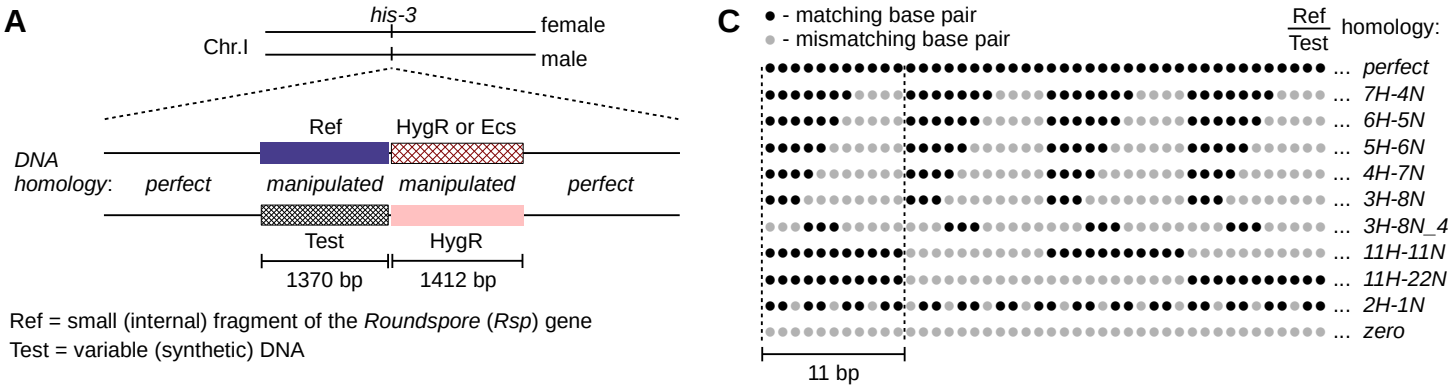

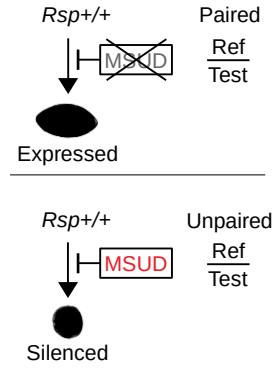

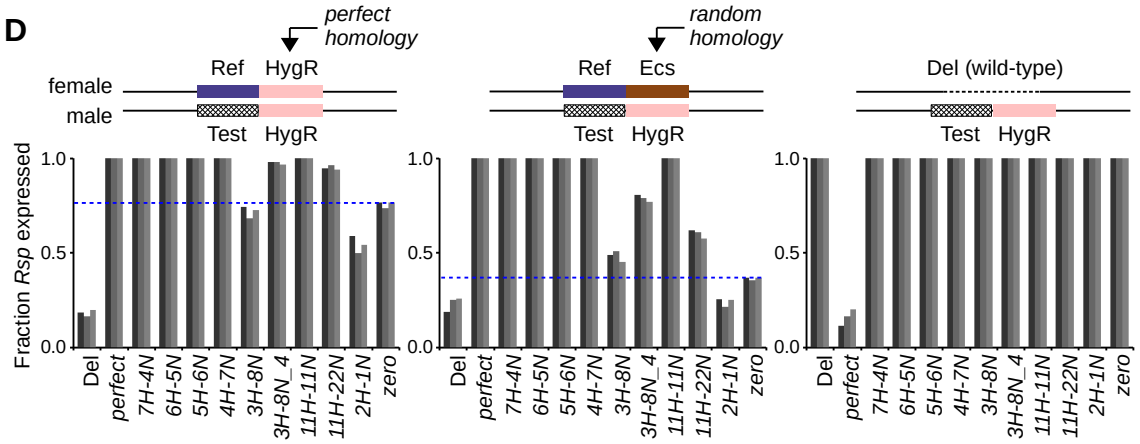

Figure 2

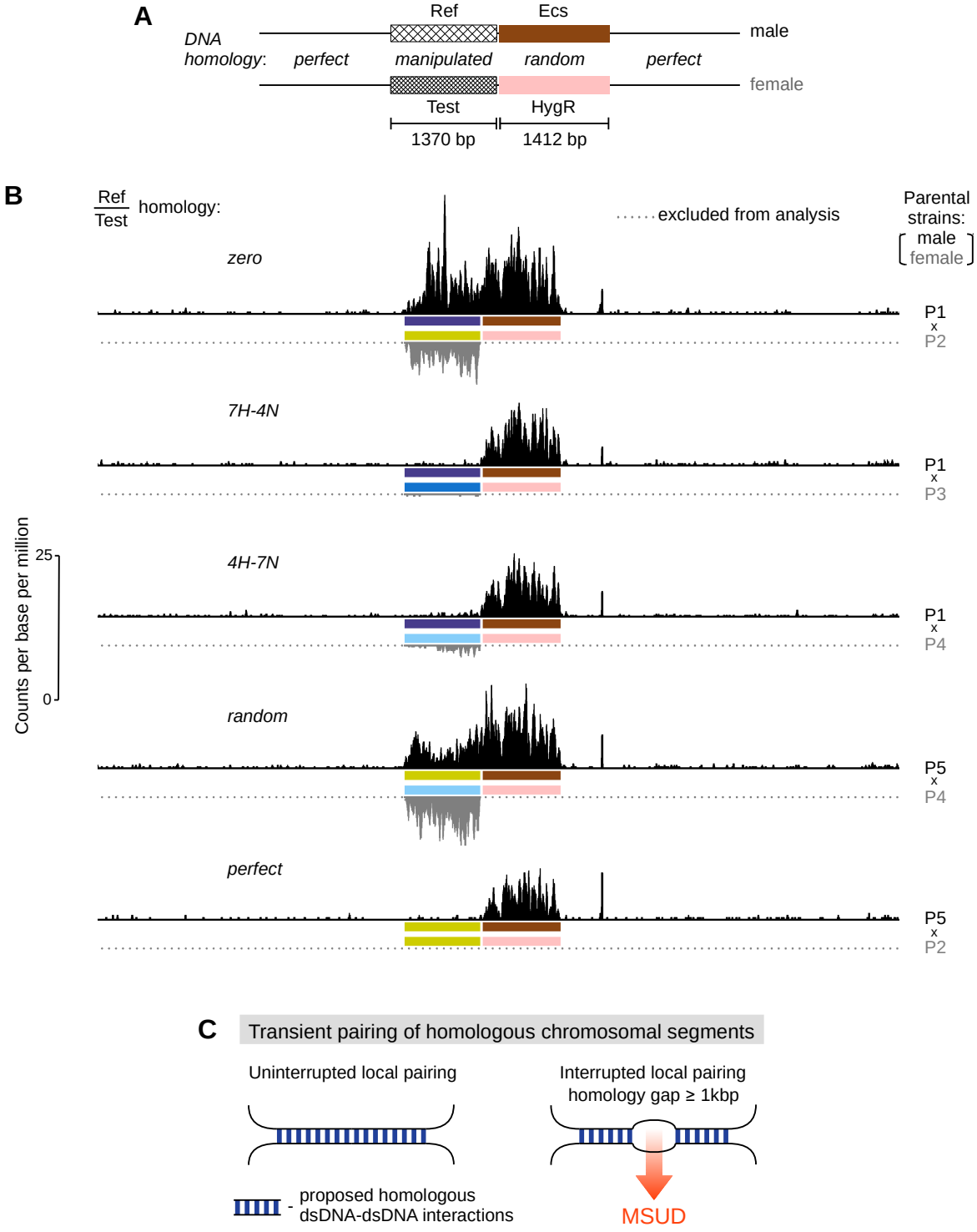

Figure 3

dim-5Δ/Δ, set-7Δ/Δ, mei-3+/Δ, spo11Δ/Δ

female

male

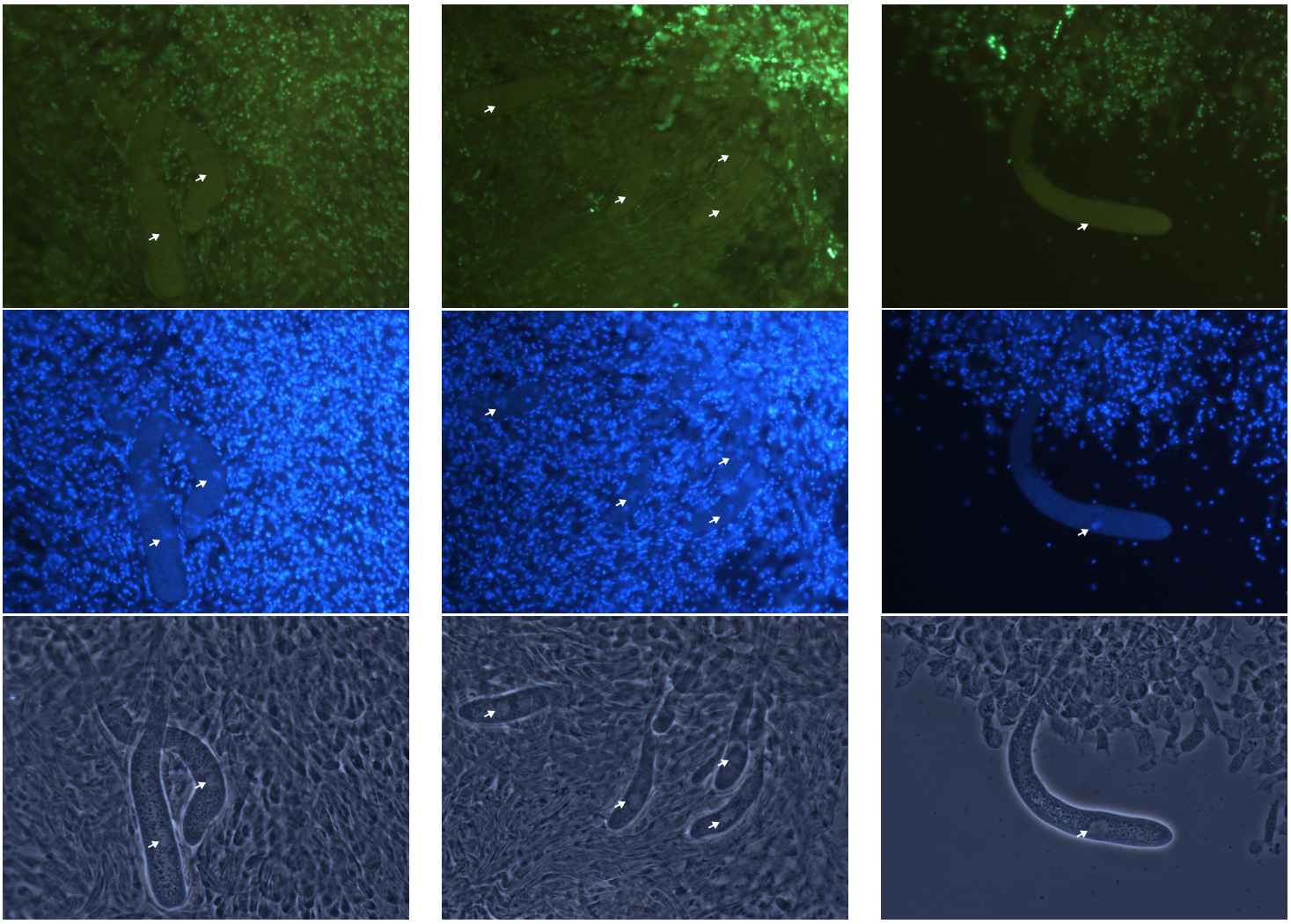

Supplementary Figure 1

A

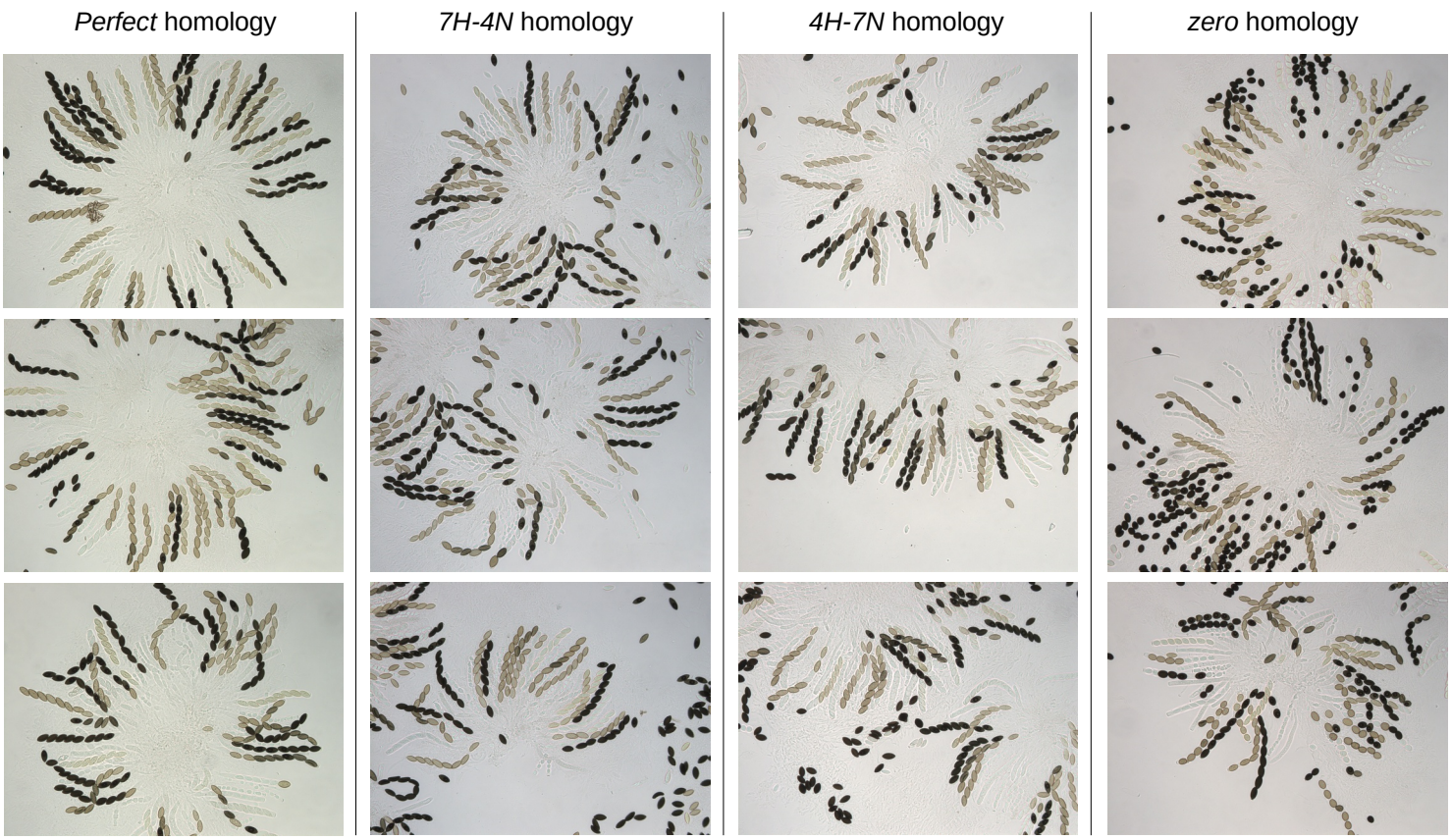

B

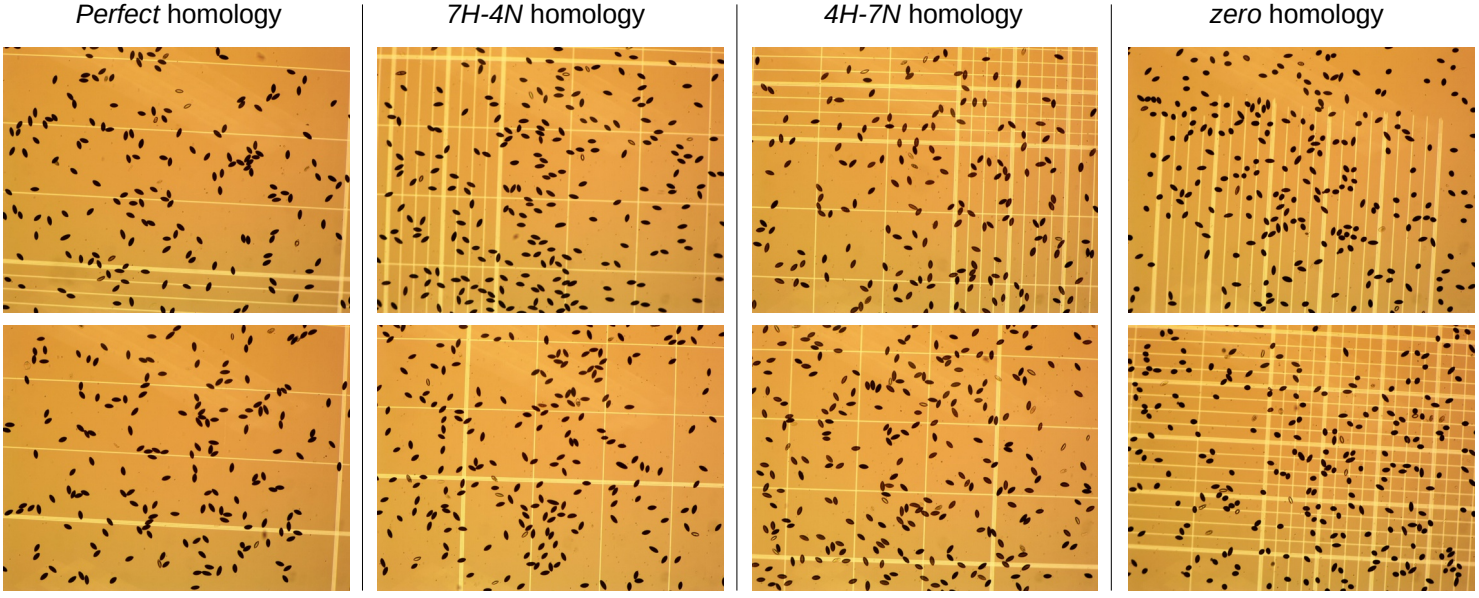

Supplementary Figure 2

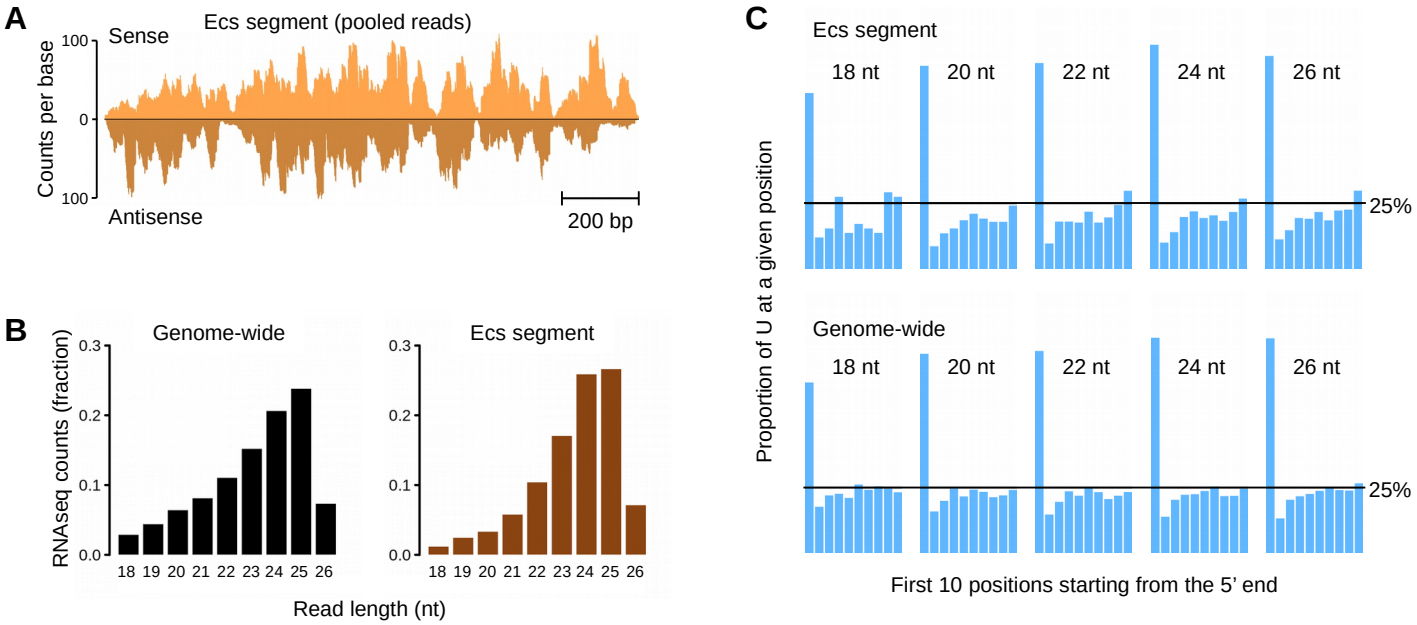

Supplementary Figure 3

Supplementary Table 1. Neurospora strains used in this study

Strain ID	Mating type	Genotype	Plasmid name	Tested locus	Allele ID	Reference
C50.3	A	*ridΔ, dim-2Δ*	N/A	*mei-3*	M0	ref. 17
C193.7	a	*ridΔ, dim-2Δ, mei-3::hH1-gfp, csr-1Δ*	pEAG258D	*mei-3*	M3	this study
C194.3	a	*ridΔ, dim-2Δ, mei-3::hH1-gfp, csr-1Δ, spo11Δ*	pEAG258D	*mei-3*	M3	this study
C196.4	A	*ridΔ, dim-2Δ, mei-3::hH1-gfp, spo11Δ*	pEAG258D	*mei-3*	M3	this study
RNR127.4	A	*ridΔ, dim-2Δ, sad-2Δ*	N/A	*mei-3*	M0	this study
RNR136.9	A	*ridΔ, dim-2Δ, mei-3Δ, spo11Δ*	N/A	*mei-3*	M1	this study
C214.1	A	*ridΔ, dim-2Δ, mei-3::hH1-gfp, spo11Δ, dim-5Δ, set-7Δ*	pEAG258D	*mei-3*	M3	this study
C223.38	a	*ridΔ, dim-2Δ, spo11Δ, dim-5Δ, set-7Δ*	N/A	*mei-3*	M0	this study
RAB10.47	a	*ridΔ, fl-, his-3+::Ref::HygR*	pTM3.1.2	*his-3*	H1	this study
RNR95.10.3	a	*ridΔ, fl-, his-3+::Ref::Ecs*	pNR74.1	*his-3*	H12	this study
RTH1005.2	a	*ridΔ, fl-, his-3+*	N/A	*his-3*	H0	ref. 35
RNR5.1	A	*ridΔ, his-3+*	N/A	*his-3*	H0	this study
RNR1.1	A	*ridΔ, his-3+::Ref::HygR*	pTM3.1.2	*his-3*	H1	this study
RNR3.2	A	*ridΔ, his-3+::7H-4N::HygR*	pSRB1	*his-3*	H2	this study
T515.1h	A	*ridΔ, his-3+::6H-5N::HygR*	pEAG254E	*his-3*	H3	this study
T514.1h	A	*ridΔ, his-3+::5H-6N::HygR*	pEAG254D	*his-3*	H4	this study
T513.1h	A	*ridΔ, his-3+::4H-7N::HygR*	pEAG254C	*his-3*	H5	this study
T511.1h	A	*ridΔ, his-3+::3H-8N::HygR*	pEAG254A	*his-3*	H6	this study
T512.1h	A	*ridΔ, his-3+::3H-8N_4::HygR*	pEAG254B	*his-3*	H7	this study
T516.1h	A	*ridΔ, his-3+::11H-11N::HygR*	pEAG254F	*his-3*	H8	this study
T517.1h	A	*ridΔ, his-3+::11H-22N::HygR*	pEAG254G	*his-3*	H9	this study
RNR4.1	A	*ridΔ, his-3+::2H-1N::HygR*	pSRB2	*his-3*	H10	this study
RNR2.3	A	*ridΔ, his-3+::zero::HygR*	pNR5.2	*his-3*	H11	this study
T544.2h	a	*ridΔ, fl-, his-3+::Ref::Ecs*	pNR74.1	*his-3*	H12	this study
T545.6h	a	*ridΔ, his-3+::zero::Ecs*	pEAG254J	*his-3*	H13	this study

Supplementary Table 2. Crosses analyzed in this study

Cross ID	Tested alleles	Homology pattern	Parental strains	
			Male	Female
X1	M0 * M2	*deletion*	C50.3	C193.7
X2	M0 * M2	*deletion*	C193.7	C50.3
X3	M0 * M2	*deletion*	RNR127.4	C194.3
X4	M0 * M2	*deletion*	C194.3	RNR127.4
X5	M1 * M2	*deletion*	RNR136.9	C194.3
X6	M1 * M2	*deletion*	C194.3	RNR136.9
X7	M2 * M2	*perfect*	C196.4	C194.3
X8	M2 * M2	*perfect*	C194.3	C196.4
X9	M0 * M2	N/A	C50.3	C194.3
X10	M0 * M2	*deletion*	C223.38	C214.1
X11	H1 * H0	*deletion*	RNR5.1	RAB10.47
X12	H1 * H1	*perfect*	RNR1.1	RAB10.47
X13	H1 * H2	*7H-4N*	RNR3.2	RAB10.47
X14	H1 * H3	*6H-5N*	T515.1h	RAB10.47
X15	H1 * H4	*5H-6N*	T514.1h	RAB10.47
X16	H1 * H5	*4H-7N*	T513.1h	RAB10.47
X17	H1 * H6	*3H-8N*	T511.1h	RAB10.47
X18	H1 * H7	*3H-8N_4*	T512.1h	RAB10.47
X19	H1 * H8	*11H-11N*	T516.1h	RAB10.47
X20	H1 * H9	*11H-22N*	T517.1h	RAB10.47
X21	H1 * H10	*2H-1N*	RNR4.1	RAB10.47
X22	H1 * H11	*zero*	RNR2.3	RAB10.47
X23	H12 * H0	*deletion*	RNR5.1	RNR95.10.3
X24	H12 * H1	*perfect*	RNR1.1	RNR95.10.3
X25	H12 * H2	*7H-4N*	RNR3.2	RNR95.10.3
X26	H12 * H3	*6H-5N*	T515.1h	RNR95.10.3
X27	H12 * H4	*5H-6N*	T514.1h	RNR95.10.3
X28	H12 * H5	*4H-7N*	T513.1h	RNR95.10.3
X29	H12 * H6	*3H-8N*	T511.1h	RNR95.10.3
X30	H12 * H7	*3H-8N_4*	T512.1h	RNR95.10.3
X31	H12 * H8	*11H-11N*	T516.1h	RNR95.10.3
X32	H12 * H9	*11H-22N*	T517.1h	RNR95.10.3
X33	H12 * H10	*2H-1N*	RNR4.1	RNR95.10.3
X34	H12 * H11	*zero*	RNR2.3	RNR95.10.3
X35	H0 * H0	N/A	RNR5.1	RTH1005.2
X36	H0 * H1	*deletion*	RNR1.1	RTH1005.2
X37	H0 * H2	*7H-4N*	RNR3.2	RTH1005.2
X38	H0 * H3	*6H-5N*	T515.1h	RTH1005.2
X39	H0 * H4	*5H-6N*	T514.1h	RTH1005.2
X40	H0 * H5	*4H-7N*	T513.1h	RTH1005.2
X41	H0 * H6	*3H-8N*	T511.1h	RTH1005.2
X42	H0 * H7	*3H-8N_4*	T512.1h	RTH1005.2
X43	H0 * H8	*11H-11N*	T516.1h	RTH1005.2
X44	H0 * H9	*11H-22N*	T517.1h	RTH1005.2
X45	H0 * H10	*2H-1N*	RNR4.1	RTH1005.2
X46	H0 * H11	*zero*	RNR2.3	RTH1005.2
X47 (“P1 x P2”)	H12 * H11	*zero*	T544.2h	RNR2.3
X48 (“P1 x P3”)	H12 * H2	*7H-4N*	T544.2h	RNR3.2
X49 (“P1 x P4”)	H12 * H5	*4H-7N*	T544.2h	T513.1h
X50 (“P5 x P4”)	H13 * H3	*random*	T545.6h	T513.1h
X51 (“P5 x P2”)	H13 * H11	*perfect*	T545.6h	RNR2.3